Separation Science and Technology
Publication details, including instructions for authors and subscription information:
http://www.informaworld.com/smpp/title~content=t713708471

A Flow-Through, Hybrid Magnetic-Field-Gradient, Rotating Wall Device for Magnetic Colloidal Separations

Alazar N. Ghebremeskel[a]; Arijit Bose[a]
[a] DEPARTMENT OF CHEMICAL ENGINEERING, UNIVERSITY OF RHODE ISLAND, KINGSTON, RHODE ISLAND, USA

To cite this Article Ghebremeskel, Alazar N. and Bose, Arijit(2000) 'A Flow-Through, Hybrid Magnetic-Field-Gradient, Rotating Wall Device for Magnetic Colloidal Separations', Separation Science and Technology, 35: 12, 1813 — 1828
To link to this Article: DOI: 10.1081/SS-100100621
URL: http://dx.doi.org/10.1081/SS-100100621

SEPARATION SCIENCE AND TECHNOLOGY, **35**(12), pp. 1813–1828, 2000

A Flow-Through, Hybrid Magnetic-Field-Gradient, Rotating Wall Device for Magnetic Colloidal Separations

ALAZAR N. GHEBREMESKEL and ARIJIT BOSE*
DEPARTMENT OF CHEMICAL ENGINEERING
UNIVERSITY OF RHODE ISLAND
KINGSTON, RHODE ISLAND 02881, USA

ABSTRACT

A 2.0 cm internal diameter 1 m long, axially-rotating horizontal glass tube, with four axially located repeating hybrid magnetic units, is used as part of a flow-through, colloidal magnetic affinity separation device. Each magnetic unit consists of an alternating current solenoid surrounding the chamber followed by four azimuthally distributed permanent magnets that rotate with the chamber. Experiments were carried out on a model feed system consisting of a mixture of 1.0 μm diameter biotinylated latex beads (targets) and 9.7 μm diameter nonfunctionalized latex beads (nontargets) at a 1:1 number ratio. Streptavidin labeled magnetic particles (2.8 μm diameter polystyrene—Dynabeads) at a number concentration of ~3×10^6 beads/mL were used as the separation vehicles. Two feed flow rates of 12 and 35 mL/min were used until a total of 600 mL of sample were processed for each. At the low rate we achieved a capture efficiency of 60 ± 4% and a separation factor of 18.2 ± 1.2 with 95 ± 4% purity. For the higher flow rate the capture efficiency was 40 ± 4% and the separation factor was 18.6 ± 1.5 with 87 ± 4% purity. A single stage batch process, where a total of 10 mL of feed was processed at identical feed and magnetic bead concentrations required ~2 hours, produced a capture efficiency of 42 ± 4% and a separation factor of 3.8 ± 1 with 79 ± 4% purity. Three batch stages (2 hours processing time per stage) were required to surpass the capture efficiency of the flow-through device at the smaller flow rate. Thus, this flow-through separation device can lead to a large increase in processing volume and reduced "down" time, compared to current batch processes, without loss of either efficiency or purity, potentially opening up magnetic colloidal separations for large scale applications.

---

* To whom correspondence should be addressed.

www.dekker.com

1. INTRODUCTION

Separation schemes where colloidal particles serve as the affinity substrates for targets in solution offer several important features that can be exploited for different applications. These include the large active surface area/volume (this quantity scales as ~1/*D*, where *D* is the particle diameter), the ability of the particles to remain in suspension by Brownian motion facilitating good mixing, and the potential to selectively mobilize target-bound particles to specific locations where they can be isolated for further processing. In colloidal magnetic affinity separation schemes, the substrates consist of ligand-coated superparamagnetic particles. Highly specific linkages between these surface-functionalized particles and target materials (either native or also surface-derivatized) are used to preferentially magnetize the targets. Steady magnetic field gradients are then employed to immobilize and then isolate these targets. The paramagnetic nature of the magnetic particles means that they can be resuspended upon removal of the external field and reused if necessary. This simple strategy has been used for cell separations (1–5), other biological macromolecules (6, 7), and for metals (8–10). Surfaces of particles containing magnetic cores can be derivatized with a large repertoire of functional groups or specific adsorbents, making this idea potentially feasible for many unexplored applications.

However, several important limitations of currently available technology have restricted the applicability of colloidal magnetic separation. These include inadequate specificity, often caused by inadequate mixing (for example, in diffusion-limited situations where the nontargets are smaller than the target macromolecules, the nontargets have higher mobility and thus have more contact with the active surfaces on the magnetic particles, creating problems if there is nonspecific binding) and the long time necessary to achieve the required degree of separation if target viability has to be maintained, because agitation can produce damaging shear forces. Since magnetic particles have specific gravities that are significantly larger than water or aqueous salt solutions, they have a tendency to sediment, and must be kept suspended by Brownian motion. This severely restricts their size, and, because the magnetic susceptibility scales with particle volume, requires use of high magnetic field gradients to mobilize them through the surrounding liquid phase at practically useful speeds. Such gradients can be produced inexpensively by introducing fine diameter soft magnetic material, such as steel wool or nickel spheres, within the solution and exposing the whole sample to a uniform magnetic field (11). However, the introduction of additional surfaces in the solution increases the potential for nonspecific binding and increases the possibility of undesirable particle trapping. Furthermore, most existing devices operate in the batch mode. This limits throughput and leads to large amounts of down time. The

Marcel Dekker, Inc.
270 Madison Avenue, New York, New York 10016

economics of this procedure have made it useful only for very high value products and processes such as cell sorting, DNA purification, protein capture, and microorganism isolation (12, 13). Technological advances that speed up this process without a concomitant loss of target specificity can make a significant impact to this burgeoning area. We have built and completed preliminary testing on a new flow-through, multiunit device that reduces separation time and increases the sample volume by two orders of magnitude without any loss of capture efficiency, target purity, and separation efficiency over an equivalent batch process. The essential features of the device are described in Section 2. Section 3 describes the experimental procedure, while the key results are described in Section 4.

2. SEPARATION DEVICE

The separation device is shown schematically in Fig. 1. It consists of a 2.0 cm internal diameter, 1.0 m long glass tube with four repeating magnetic units. Each unit consists of a stationary alternating current solenoid that surrounds the tube, followed by two pairs of 1 kGauss Al-Ni-Co magnets positioned azimuthally on the tube at a distance of 2.0 cm from the end of the solenoid. Each permanent magnet pair consists of magnets at diametrically opposite ends, the second pair being located 1.0 cm downstream from the first, and positioned at

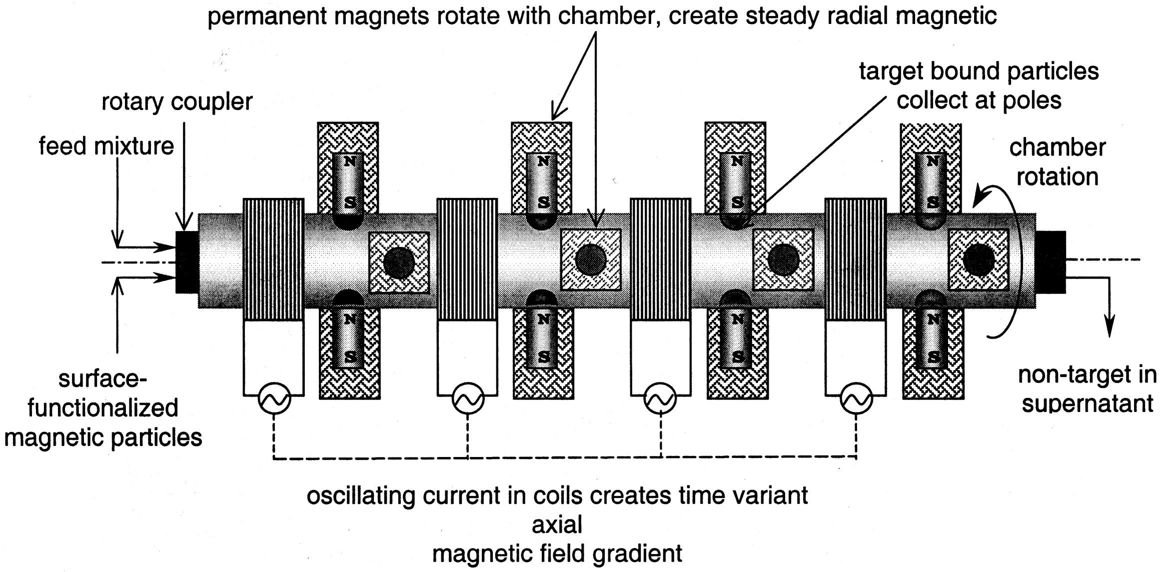

FIG. 1 Schematic representation of the 2.0 cm internal diameter 1 m long axially rotating horizontal chamber with four repeating magnetic units. Each unit consists of a stationary alternating current solenoid surrounding the chamber followed by two pairs of azimuthally distributed permanent magnets that rotate with the chamber.

90° to the first. The tube axis is horizontal, and the chamber rotates about this axis at ~25 rpm. The slow rotation simulates a low-gravity environment within the chamber and significantly reduces sedimentation of nonneutrally buoyant particles without introducing centrifugal forces, a critical feature of this device. The permanent magnets rotate with the tube. Separate peristaltic pumps drive the feed mixture and the magnetic colloid suspension through a rotary coupler (Deublin Inc.) into one end of the chamber. A second rotary coupler at the other end of the chamber allows the exiting liquid to flow into a stationary collection vessel.

Each solenoid has 14 turns of copper wire over a length of 2.5 cm has a diameter of 2.5 cm, and carries an alternating current of amplitude 10 A at a frequency of 60 Hz. As the particles and feed mixture flow through the chamber, they are first acted upon by the magnetic field gradient produced by the solenoid. For a magnetic particle entering the solenoid, the axial component of the magnetic field gradient varies in magnitude as the current changes but points in the same direction as the base flow. Along the axis of a solenoid of radius R and length L, this field B is given by

$$B(x) = \mu_0 NI[\{x + L/2\}\{R^2 + (x + L/2)^2\}^{-1/2} - \{x - L/2\}\{R^2 + (x - L/2)^2\}^{-1/2}]/2L \qquad (1)$$

where x is measured from the center of the solenoid, N is the number of turns, I is the current, and μ_0 is the permeability of free space. The local field and field-gradient impart a time-varying axial force on the paramagnetic 2.8 μm diameter Dynabead particles, inducing particle motion through the surrounding liquid beyond that produced by the base flow. As an illustration of this effect, the solenoid-current-induced transient velocities for a magnetic bead positioned at the solenoid entrance $x = -L/2$ and on the axis, calculated using Stokes' law (particle magnetization data provided by Dynal Corp.) and Eq. (1) are shown in Fig. 2. The maximum induced velocity is ~60 μm/s. As the particle moves toward the center of the solenoid, the axial magnetic force reduces. Past the midpoint, the direction of the time-varying axial magnetic field gradient reverses, creating a particle velocity opposite to the base flow. Because the length/diameter ratio of the solenoid is ~1, fringing effects dominate and no location within the solenoid has a uniform axial magnetic field, as shown in Fig. 3. This minimizes magnetically "dead" regions within the separation chamber. The radial component of the magnetic field within the solenoid is also nonuniform. Thus each particle also experiences a time-varying radial force that results in local radial motion. In addition, the time varying magnetic field induces an oscillating torque on each particle. The expected consequence of the alternating current in the solenoid is a transient motion of the particles superimposed on a steady one imposed by the base flow, thus enhancing the mixing within the chamber without introducing additional sur-

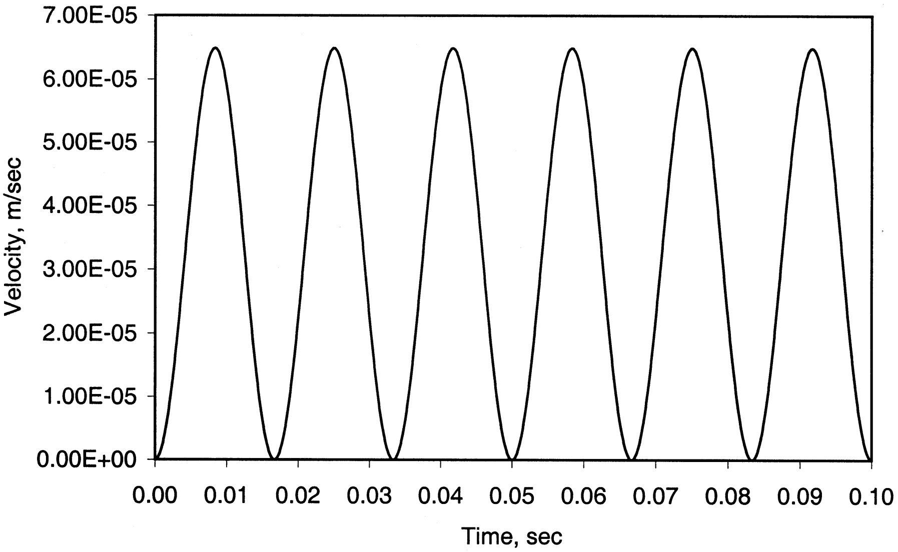

FIG. 2 Axial velocities induced by the alternating current for a magnetic particle located at the entrance of the solenoid and on the axis of the chamber, calculated using Stokes' law and particle magnetization data provided by the manufacturer. The induced velocities would differ in direction at the solenoid exit. These velocities, along with a radial component not shown as well as a torque-induced rotary oscillation, superimpose on the particle motion created by the base flow and result in micromixing.

faces within it. (*Note*: The base flow has a nonzero vorticity which adds to rotary motion of the particles.)

In the absence of any magnetic forces, the residence time for particles in the chamber for the flow rates used is of the order of a few minutes. The perma-

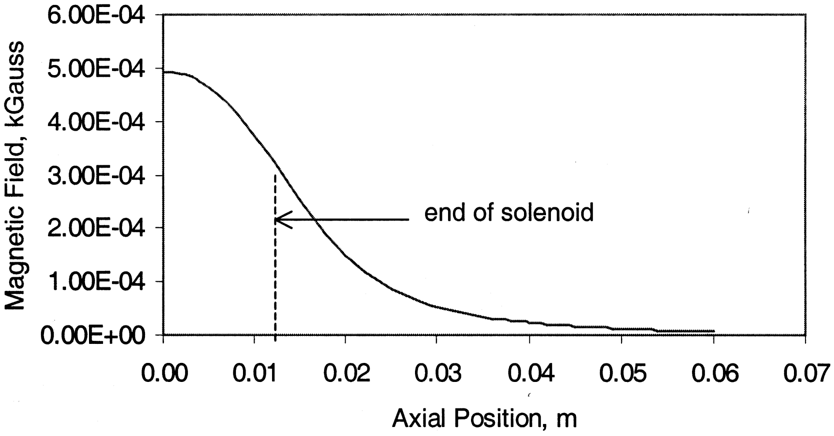

FIG. 3 Magnetic field versus position in the solenoid. Solenoid diameter 2.5 cm, length 2.5 cm, current 10 A. No location within the solenoid has a uniform axial magnetic field, thus excluding magnetically dead regions from the chamber.

nent magnet strength must be enough to permit target particles to move a distance equal to the tube radius in a time that is short compared to this residence time. Using Stokes' law, a force of ~$1.6 \times 10^{-3}D$ dynes is needed to move a particle of diameter D cm at a radial velocity of 0.1 cm/s (this would mean 10 seconds for a particle at the axis to reach the wall) through a liquid of water-like viscosity. For the 2.8 μm Dynabeads used in our experiments, the magnetic field gradient required to create this force is ~0.5 kGauss/cm. Figure 4 shows the experimentally measured field as a function of radial position along the diameter connecting two facing Al-Ni-Co permanent magnets, and demonstrates that these magnets are strong enough to move the particles to the wall well within the required time.

The trajectory taken by a magnetic particle entering the device is affected by the geometry of the system, including the placement of the solenoids and permanent magnets and the direction of the flow. Figure 5 is a qualitative representation of the forces acting on a particle as it moves through the device. (*Note*: Gravity and centrifugal forces are ignored because of the slow rotation of the device about a horizontal axis.) In Region A, the particle is far from the influence of the solenoid or the permanent magnets. It moves along a streamline at a constant velocity corresponding to the base flow, so that there are no forces acting on it. In Region B, still far from the influence of the permanent magnets, the particle experiences an axial force created by the solenoid and a drag force in the opposite direction. In Region C, the influence of the permanent magnets becomes important, and the effect of the solenoid is negligible. The particle then experiences a radial force, which is opposed by drag. It is

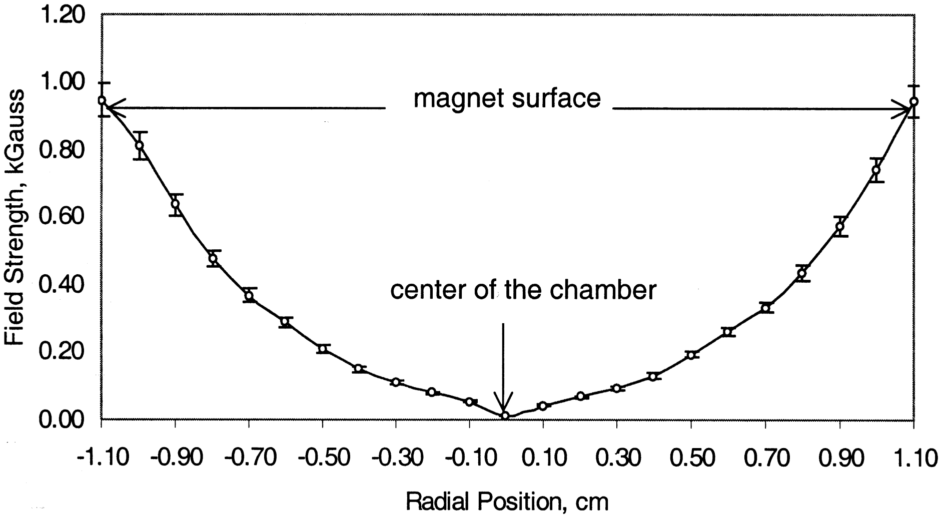

FIG. 4 Magnetic field versus radial position for the Al-Ni-Co permanent magnets arranged at diametrically opposite ends of the chamber. The field gradient is ~1 kGauss/cm.

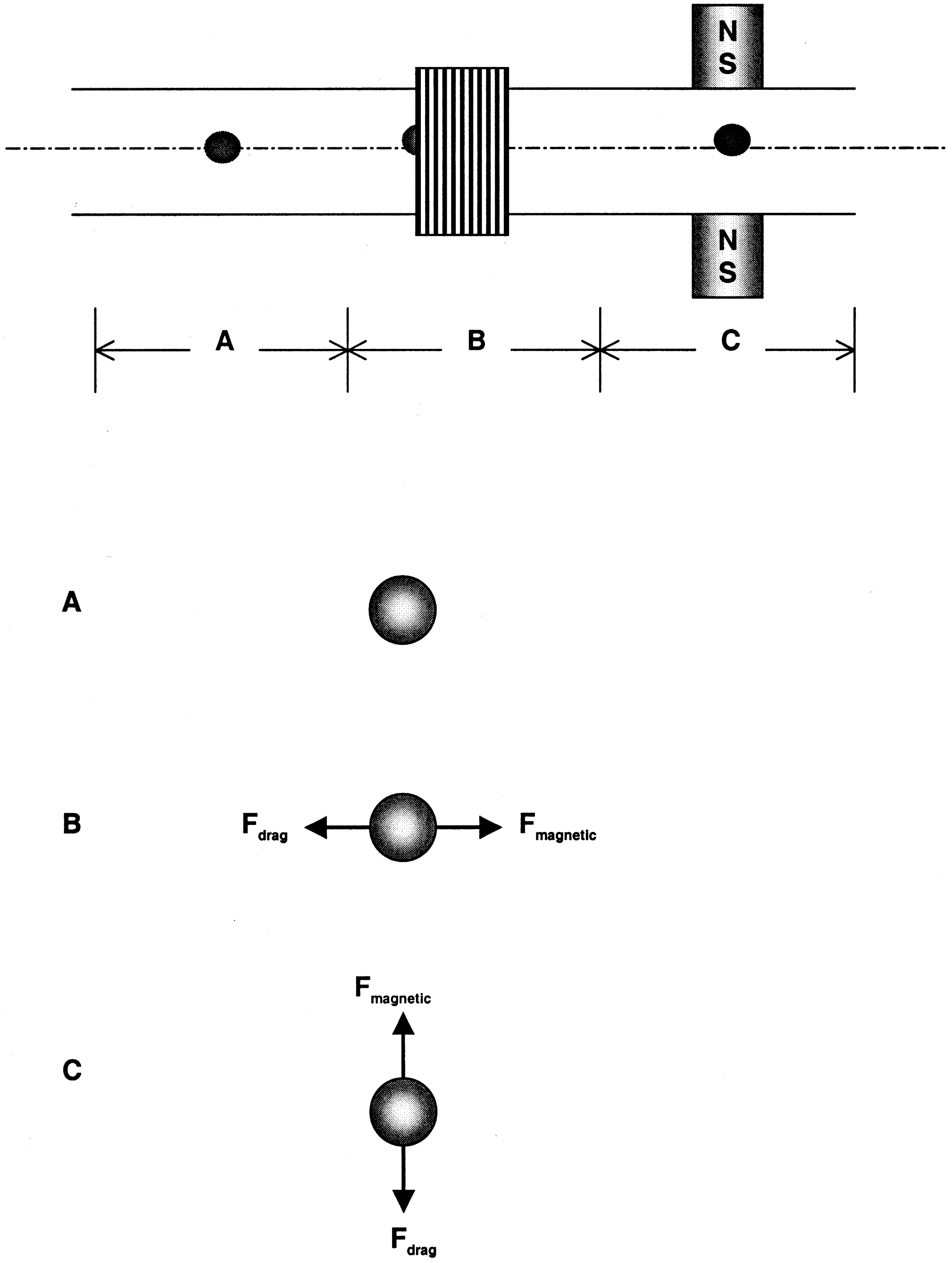

FIG. 5 The forces acting on a magnetic particle as it moves through the device. *Region A*: This region is "far" from the influence of the solenoid and the permanent magnets. The particle moves along a streamline at a constant velocity set by the base flow, and no forces act on it. (*Note*: The characteristic time required for a particle entering the device to achieve terminal velocity is $\sim m/\mu D$, where m is the mass of the particle, D is its diameter, and μ the liquid viscosity. This is of the order of a few microseconds for a Dynal magnetic particle.) *Region B*: Here the particle experiences an axial force created by the solenoid, and an opposing drag force. It is not influenced by the permanent magnets. *Region C*: The permanent magnets induce a radial magnetic force. An opposing drag force is also created. This region is far from the solenoid. Particles leave the streamlines in Region C, and are captured on the tube walls.

only in Region C that the particle trajectory deviates from the streamline, allowing capture at the tube wall.

3. EXPERIMENTAL PROCEDURE

M-280 (2.8 μm diameter) streptavidin coated magnetic beads were obtained from Dynal Inc. These beads have a specific gravity of 1.3, so they would sediment rapidly if left unperturbed in an aqueous solution. The target particles were 1 μm diameter biotin-labeled polystyrene beads (Sigma Chemical Company) while the nontarget particles were 9.7 μm diameter nonfunctionalized but charge-stabilized polystyrene particles (Interfacial Dynamics Corporation). Both the target and nontarget particles are essentially neutrally buoyant. Single distilled water was passed through a four cartridge Millipore "Mill Q" system until its resistivity reached 18 MΩ-cm. This water was used for preparing all the suspensions.

The streptavidin beads were used at a particle number concentration of ~3×10^6 beads/mL. All particle concentrations are measured in a hemocytometer mounted on a Nikon optical microscope. The feed consisted of biotinylated polystyrene beads mixed in a 1:1 number ratio with the nonfunctionalized beads at an overall particle number concentration of ~6×10^4/mL. 100 mL of the magnetic beads and an equal volume of a sample containing the target and nontarget material were fed simultaneously at two different flow rates specified below. The target and nontarget particles were sufficiently different in size so that they could be easily distinguished using optical microscopy.

In a typical experiment (some control experiments were also performed, where the chamber was not rotated, or there was no current in the solenoid), the chamber is first filled with distilled water using the peristaltic pumps. The feed and magnetic particle flows are then initiated, along with chamber rotation and current in the solenoids. The liquid flowing out through the end of the chamber, called the supernatant, is collected continuously. When the appropriate liquid volume is collected (usually 600 mL), the flow of the feed and magnetic particle suspensions is interrupted and the total volume of feed that has entered the chamber is recorded. The right end of the chamber is then opened, and the remaining supernatant allowed to flow out and is added to that already collected. The chamber is then closed, and 500 mL of distilled water is pumped through, flushing out all the particles in the supernatant. This material is also added to the already collected liquid. The number concentrations of target particles in the feed and the supernatant are multiplied by the total feed and supernatant volumes to obtain the number of particles in the feed (N_{fT}) and in the supernatant (N_{ST}). Similarly, the number of nontarget particles in the feed and supernatant, N_{fN} and N_{SN}, respectively, are obtained. The particle capture efficiency, η, is evaluated using

$$\eta = 100(N_{\mathrm{fT}} - N_{\mathrm{ST}})/N_{\mathrm{fT}} \tag{2}$$

The permanent magnets are then removed, and distilled water is allowed to flow through the chamber. The magnetic particle/target complexes that had been immobilized at the chamber walls are now resuspended into the chamber, and driven out from the other end by the bulk flow. The magnetic-particle-rich solution collected in this way is designated as the suspension from the pole region. The exact counting of target particles from this suspension proved difficult because it was hard to distinctly identify individual ones when they were clustered around the magnetic beads. Thus an indirect, mass balance approach was used, with the target particle number percent at the pole region, X_{T}, being given by

$$X_{\mathrm{T}} = 100(N_{\mathrm{fT}} - N_{\mathrm{ST}})/\{(N_{\mathrm{fT}} - N_{\mathrm{ST}}) + (N_{\mathrm{fN}} - N_{\mathrm{SN}})\} \tag{3}$$

The number percent of targets in the supernatant, Y_{T}, is obtained directly from

$$Y_{\mathrm{T}} = 100N_{\mathrm{ST}}/(N_{\mathrm{ST}} + N_{\mathrm{SN}}) \tag{4}$$

The quantity X_{T} is a measure of the purity of the target material at the poles. The separation factor, β, is then calculated using

$$\beta = \{X_{\mathrm{T}}/(100 - X_{\mathrm{T}})\}/\{Y_{\mathrm{T}}/(100 - Y_{\mathrm{T}})\} \tag{5}$$

The numbers reported represent an average from five experiments, with five samples withdrawn from each region for each experiment. Clearly β must be different from 1 for the separation to be successful.

4. RESULTS AND DISCUSSION

Experiments were performed to confirm that the rotation of the chamber and the alternating current in the solenoid are indeed crucial for the separation. Two overall feed flow rates were used: 12 and 35 mL/min, and a total of 600 mL of sample was processed. The capture efficiencies for all of the experimental conditions are shown in Fig. 6. For the conditions probed in these experiments, the first magnetic unit was located 40.0 cm downstream from the entrance of the chamber. In the experiment with no chamber rotation, nearly all of the magnetic particles sedimented before arriving at the first magnetic unit, while most of the target particles exited through the end of the chamber, leading to the extremely low capture efficiency. Introduction of the alternating current in the solenoid enhances the capture efficiencies, nearly doubling it for the lower flow rate, and increasing it by a factor of 50% for the higher flow rate. A dramatic increase in efficiency is observed for both flow rates when rotation is initiated, clearly pointing to the impor-

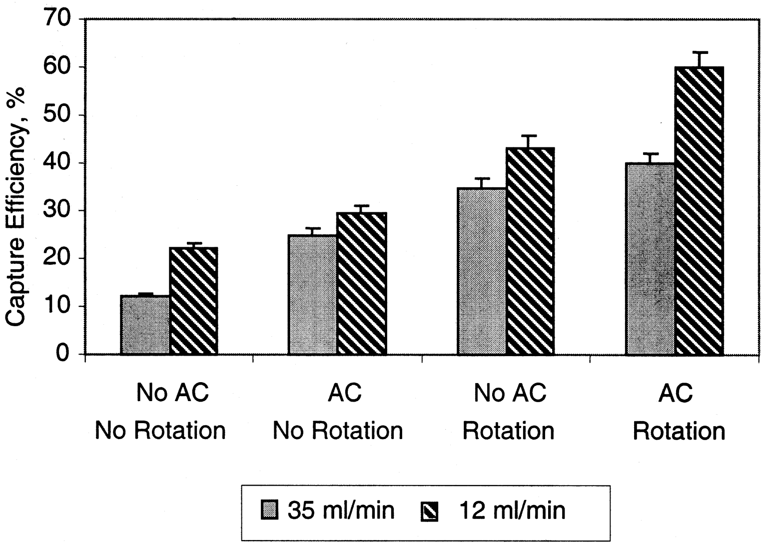

FIG. 6 Capture efficiencies for the four-magnetic unit device at two feed flow rates, 12 and 35 mL/min. The enhancements produced by current flowing in the solenoids as well as chamber rotation are apparent.

tant consequence of keeping the magnetic particles suspended in solution and promoting contact with the neutrally-buoyant targets. When both the mixing caused by the current in the solenoid as well as chamber rotation are included, the average capture efficiencies reach 40 and 60% for the higher and lower flow rates, respectively.

The importance of each magnetic unit toward the overall capture efficiency was examined by starting with one (consisting of the solenoid and four permanent magnets) and sequentially adding the others. The results, for a flow rate of 12 mL/min are shown in Fig. 7. One unit gives a capture efficiency of 22%. Each additional unit produced a further separation of the target molecules, up to a level of 60% when all four are in place. These capture efficiencies are not sensitive to the exact positions of each of the magnetic units, indicating that chamber rotation is effective in keeping the magnetic particles in suspension.

At this flow rate the separation factors β as each of the repeating units is added are shown in Fig. 8. One unit produces a separation factor ~3.4. As the other units are added, the monotonic drop in Y_T causes the separation factor to rise systematically to an average final value of 18.2. The average separation factor achieved at the higher flow rate was 18.6. Note that this device is equivalent to a single-stage unit from the perspective of a cocurrent separation scheme. This dramatically high separation factor can clearly be exploited in a multistage cascade, each stage consisting of the chamber described here. Furthermore, the judicious use of reflux can provide significant additional benefits for separation.

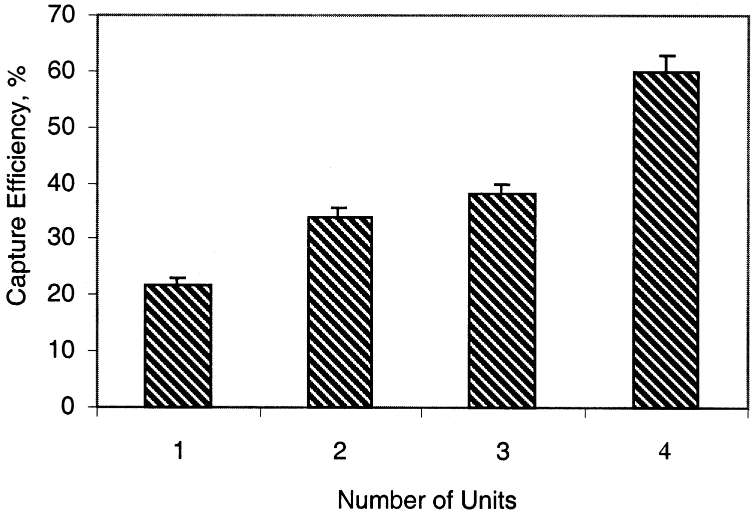

FIG. 7 Capture efficiencies versus total number of magnetic units at a feed flow rate of 12 mL/min.

We obtained the purity of the target material at the pole region (number concentration of targets divided by the total number concentration of target and nontarget) for each flow rate studied. Figure 9 shows results for the lower flow rate—a 95% purity for the model system used in this study. At the higher flow rate the purity was 81%. As discussed later, the concentration of nontarget particles in the pole regions is not caused by nonspecific binding, but rather is a physical particle trapping effect.

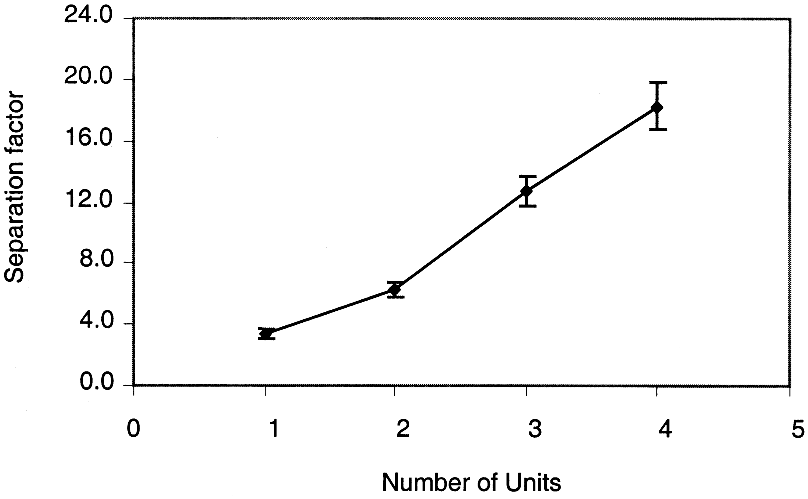

FIG. 8 Separation factor versus total number of magnetic units for a feed flow rate of 12 mL/min. The drop in the target particle number concentration in the supernatant is responsible for the rise in separation factor as each unit is added.

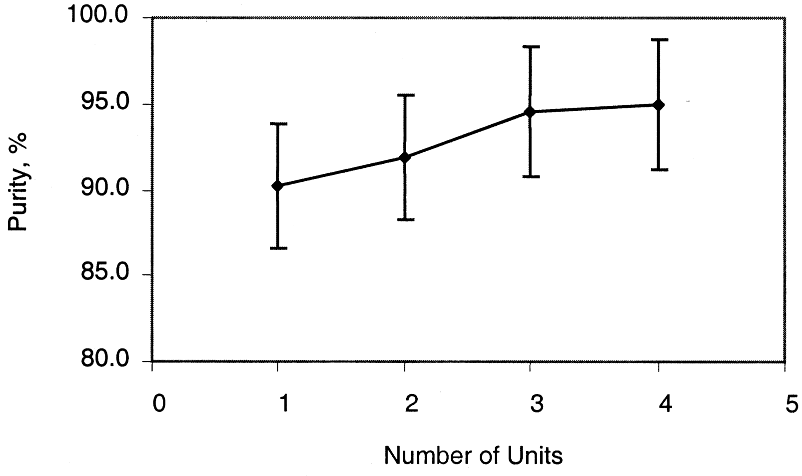

FIG. 9 Target purity versus total number of units for a feed flow rate of 12 mL/min. The purity of the target material is not affected by the number of magnetic units and remains at ~95%.

The efficacy of this flow-through device can be evaluated by comparing its performance with a batch processing scheme, shown schematically in Fig. 10. To make a meaningful comparison, the processing was done in a vial of diameter 2.0 cm, and the same set of Al-Ni-Co permanent magnets was used. All concentrations were similar to those utilized for the flow-through experiments in our device. Thus, the biotinylated polystyrene beads were mixed in a 1:1 number ratio with nonfunctionalized beads and ~3×10^6 beads/mL of streptavidin coated magnetic beads at an overall particle number concentration of ~6×10^4/mL. The total sample volume was 10 mL. This volume limit was dictated by the amount of time required for the magnetic particles to collect at the poles after application of the field gradient. The suspension is shaken continuously for 1 hour, then exposed to the permanent magnets for 45 minutes. Placement of the magnet near the top of the tube moves the magnetized target particles, concentrating them at the poles, while the supernatant region contains the nontarget particles. Samples are then withdrawn from both the supernatant as well as the pole region, and target and nontarget particle concentrations counted in a hemocytometer. Figure 11 shows the capture efficiencies for each stage in a three-stage scheme. A single batch stage gives a capture efficiency of 42%, far lower than the 60% efficiency in our device at a flow rate of 12 mL/min and comparable to that obtained in our device for the higher flow rate. The separation factor β for a single batch stage is 3.4, much lower than the factor of ~18 in our device. In addition, the purity obtained here is 79%, also comparable to that in our flow-through device. Note that we needed three batch stages, each requiring ~2 hours of operation, to get the capture efficiency beyond that in our device at the lower flow rate.

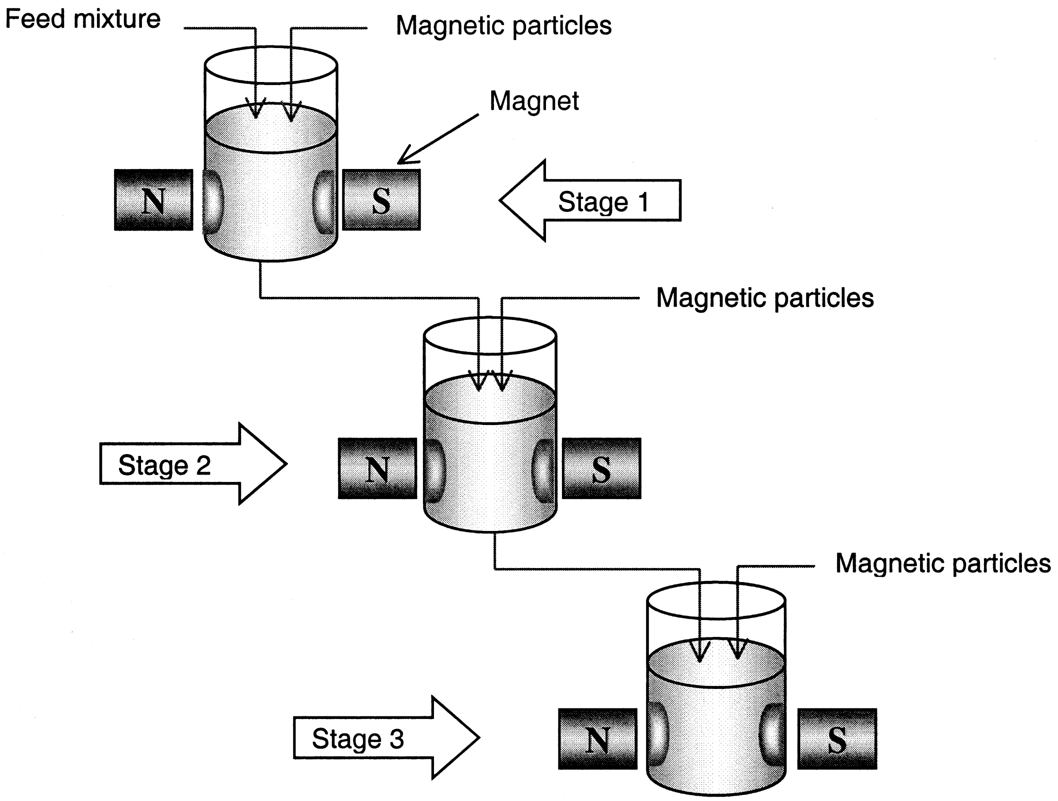

FIG. 10 The arrangement used in the laboratory for applying the magnetic field gradient for multistage batch processing. Magnetic particles are added to the test tube containing the mixture of target and nontarget molecules, and shaken continuously for ~1 hour. A pair of the Al-Ni-Co magnets are then placed near the top of the tube, and the magnetized target particles are allowed to concentrate at the poles for 45 minutes. The supernatant contains most of the nontarget particles. Samples are then withdrawn from both the supernatant as well as the pole region for analysis.

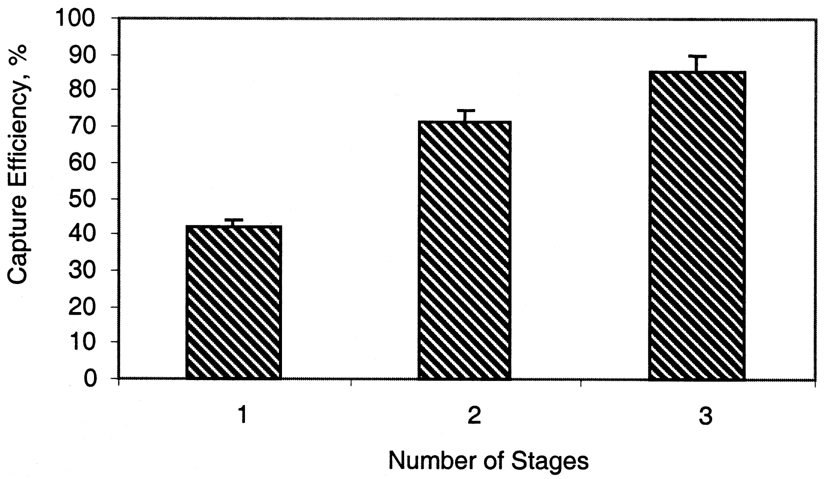

FIG. 11 Capture efficiencies versus number of stages for the batch process. Note that three batch stages are required to surpass the capture efficiency of our device at a flow rate of 12 mL/min.

A part of the difference between the performance of our device and a batch process can be understood by examining the material that collects at the poles for each. These are shown in Fig. 12. The cluster size for the flow-through device is routinely smaller than that in batch units. This is a consequence of particle motion created by the flow, as well as the magnetic field gradients. The smaller clusters lead to a larger available surface area per unit volume, and lead to better capture efficiencies.

In order to examine the extent of nonspecific binding, some control batch experiments were conducted. The nontarget particles were incubated with the streptavidin beads for 2 hours. The Al-Ni-Co magnets were then used to concentrate the magnetic particles, samples were withdrawn from this concentrated region, gently diluted, and examined by optical microscopy. While an extremely small number of nontarget particles were detected, none were attached to the magnetic beads. Thus we see no experimental evidence of nonspecific binding. The loss of purity is therefore a consequence of trapping of the nontarget particles by clusters of the magnetic beads as they travel toward the poles of the permanent magnets, a physical rather than a chemical effect.

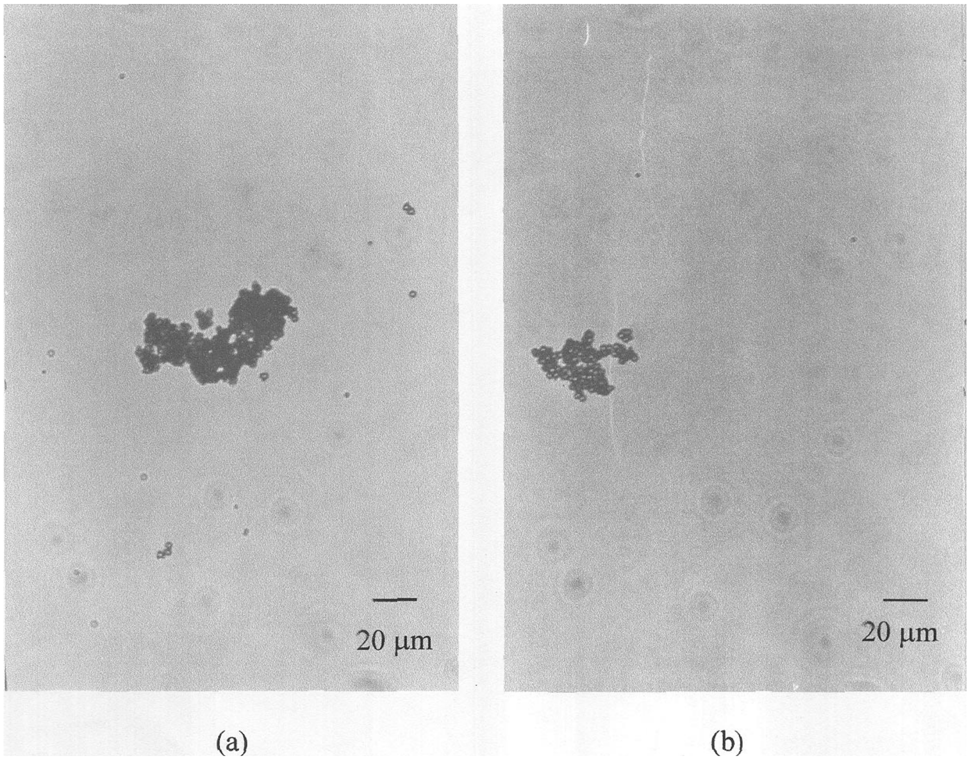

FIG. 12 Optical micrograph showing clusters from the pole region in (a) the batch device and (b) the flow-through device. The cluster sizes for the flow-through device are smaller, allowing more surface area to be available for target attachment.

Our experimental results using a model system indicate that this flow-through multiunit separation device can lead to a large increase in processing volume and reduced “down” time compared to current batch processes, without a significant reduction in either efficiency or purity, potentially opening up magnetic colloidal separations for medium and large-scale applications. The mode of operation currently demonstrated would apply directly to a negative selection strategy, where the nontarget particles are the ones of interest and are collected primarily in the supernatant, or the target particles are contaminants that need to be removed from a large volume of solution.

5. CONCLUSIONS

A new flow-through, multimagnetic-unit device, consisting of a slowly rotating horizontal chamber, has been designed and demonstrated for colloidal magnetic affinity separation. Each magnetic unit consists of an alternating-current-carrying solenoid surrounding the chamber, and two pairs of permanent magnets located downstream from the solenoid, that rotate with the chamber. The chamber rotation simulates a low gravity environment, severely attenuating any sedimentation of nonneutrally buoyant magnetic particles as well as feed, thus promoting good particle–target contact throughout the chamber volume. The oscillating magnetic field gradient produced by the solenoid introduces translational and rotary microparticle oscillations, enhancing mixing, while the permanent magnets immobilize the targets on the chamber walls. For a model feed system consisting of a ~50% mixture of biotinylated latex beads (target) and nonfunctionalized latex beads (nontarget), we have been able to achieve a maximum separation capture efficiency of 60% and a separation factor of ~18.2 with purity as high as 95%. The total feed volume we processed was 600 mL at a flow rate of 12 mL/min. At a flow rate of 35 mL/min the capture efficiency was reduced to 40%, but without a significant change in the separation factor or purity. A single-stage batch process using the same particle concentrations required 2 hours, and gave a capture efficiency of 42%, a separation factor of 3.8, and a purity of 80%. Three batch stages were required to surpass the low flow rate capture efficiency of our device. These results show the potential of this device for magnetic colloidal separation at medium and large scales.

ACKNOWLEDGMENTS

Financial support for this work was provided by the National Science Foundation (CTS 9618635) and the University of Rhode Island Foundation. We thank A. C. Nunes for several useful discussions.

REFERENCES

1. A. J. Richards, O. S. Roath, R. J. S. Smith, and J. H. P. Watson, *IEEE Trans. Magn., 32*, 460 (1996).
2. A. S. Bahaj, P. A. B. James, and F. D. Moeschler, *Ibid., 32*, 5106 (1996).
3. J. M. Van der Wolf, J. R. C. M. Van Beckhoven, Ph. M. de Vries, and J. W. L. Van Vuurde, *J. Appl. Bacteriol. 77*, 160 (1994).
4. T. E. Thomas and P. M. Lansdorp, *Prog. Clin. Biol. Res., 389*, 65 (1994).
5. J. J. Chalmers, M. Zborowski, L. Sun, and L. R. Moore, *Biotechnol. Prog., 14*, 141 (1998).
6. I. Safarík, M. Safaríková, and S. J. Forsythe, *J. Appl. Bacteriol. 78*, 575 (1995).
7. G. Kapperud, T. Vardunt, E. Skjerve, E. Hornes, and T. E. Michaelsen, *Appl. Environ. Microbiol., 59*, 2938 (1993).
8. A. D. Ebner, J. A. Ritter, H. J. Ploehn, R. L. Kochen, and J. D. Navratil, *Sep. Sci. Technol.*, *34,* 1277 (1999).
9. L. Nuñez and M. D. Kaminski, *Chemtech, 28*, 41 (1998).
10. L. Nuñez, B. A. Buchholz, and G. F. Vandergrift, *Sep. Sci. Technol.*, *30*, 1455 (1995).
11. J. H. P. Watson, in L. Svarovsky (Ed.), *Solid-Liquid Separation: High Gradient Magnetic Separation*, 3rd ed., Butterworth-Heinemann, Oxford, 1990.
12. B. I. Haukanes and Kvam, *Bio/Technology, 11*, 60 (1993).
13. O. Olsvik, T. Popovic, E. Skjerve, K. Cudjoe, E. Hornes, J. Ugelstad, and M. Uhlén, *Clin. Microbiol. Rev., 7*, 43 (1994).

Received by editor August 19, 1999
Revision received January 2000

Downloaded At: 10:56 25 January 2011

Request Permission or Order Reprints Instantly!

Interested in copying and sharing this article? In most cases, U.S. Copyright Law requires that you get permission from the article's rightsholder before using copyrighted content.

All information and materials found in this article, including but not limited to text, trademarks, patents, logos, graphics and images (the "Materials"), are the copyrighted works and other forms of intellectual property of Marcel Dekker, Inc., or its licensors. All rights not expressly granted are reserved.

Get permission to lawfully reproduce and distribute the Materials or order reprints quickly and painlessly. Simply click on the "Request Permission/Reprints Here" link below and follow the instructions. Visit the U.S. Copyright Office for information on Fair Use limitations of U.S. copyright law. Please refer to The Association of American Publishers' (AAP) website for guidelines on Fair Use in the Classroom.

The Materials are for your personal use only and cannot be reformatted, reposted, resold or distributed by electronic means or otherwise without permission from Marcel Dekker, Inc. Marcel Dekker, Inc. grants you the limited right to display the Materials only on your personal computer or personal wireless device, and to copy and download single copies of such Materials provided that any copyright, trademark or other notice appearing on such Materials is also retained by, displayed, copied or downloaded as part of the Materials and is not removed or obscured, and provided you do not edit, modify, alter or enhance the Materials. Please refer to our Website User Agreement for more details.

Order now!

Reprints of this article can also be ordered at
http://www.dekker.com/servlet/product/DOI/101081SS100100621